



Published in final edited form as:

Dev Biol. 2015 March 1; 399(1): 15–26. doi:10.1016/j.ydbio.2014.11.026.

Asymmetric Expression of Connexins between luminal epithelial- and myoepithelial- cells is Essential for Contractile Function of the Mammary Gland

Rana Mroue³, Jamie Inman¹, Joni Mott¹, Irina Budunova², and Mina J. Bissell^{1,*}

¹Life Sciences Division, Lawrence Berkeley National Laboratory, Berkeley CA 94720

²Department of Dermatology, Northwestern University Feinberg School of Medicine, 676 North St. Clair Street, Suite 1600, Chicago, IL 60611

³Helen Diller Family Cancer Research Center, UCSF, 1450 3rd street, San Francisco CA 94158

Abstract

Intercellular communication is essential for glandular functions and tissue homeostasis. Gap junctions couple cells homotypically and heterotypically and coordinate reciprocal responses between the different cell types. Connexins (Cx) are the main mammalian gap junction proteins, and the distribution of some Cx subtypes in the heterotypic gap junctions is not symmetrical; in the murine mammary gland, Cx26, Cx30 and Cx32 are expressed only in the luminal epithelial cells and Cx43 is expressed only in myoepithelial cells. Expression of all four Cxs peaks during late pregnancy and throughout lactation suggesting essential roles for these proteins in the functional secretory activity of the gland. Transgenic (Tg) mice over-expressing Cx26 driven by keratin 5 promoter had an unexpected mammary phenotype: the mothers were unable to feed their pups to weaning age leading to litter starvation and demise in early to mid-lactation. The mammary gland of K5-Cx26 female mice developed normally and produced normal levels of milk protein, suggesting a defect in delivery rather than milk production. Because the mammary gland of K5-Cx26 mothers contained excessive milk, we hypothesized that the defect may be in an inability to eject the milk. Using ex vivo three-dimensional mammary organoid cultures, we showed that tissues isolated from wild-type FVB females contracted upon treatment with oxytocin, whereas, organoids from Tg mice failed to do so. Unexpectedly, we found that ectopic expression of Cx26 in myoepithelial cells altered the expression of endogenous Cx43 resulting in impaired gap junction communication, demonstrated by defective dye coupling in mammary epithelial cells of Tg mice. Inhibition of gap junction communication or knock-down of Cx43 in organoids from wild-type mice impaired contraction in response to oxytocin, recapitulating the observations from the mammary glands of Tg mice. We conclude that Cx26 acts as a trans-dominant negative for Cx43 function in myoepithelial cells, highlighting the importance of cell type-specific expression of Cxs for optimal contractile function of the mammary myoepithelium.

*Corresponding Author: mailing address Lawrence Berkeley National Laboratory, One Cyclotron Rd MS 977 Berkeley, CA 94720
Phone: (510) 486-4365. MJBissell@lbl.gov.

Publisher's Disclaimer: This is a PDF file of an unedited manuscript that has been accepted for publication. As a service to our customers we are providing this early version of the manuscript. The manuscript will undergo copyediting, typesetting, and review of the resulting proof before it is published in its final citable form. Please note that during the production process errors may be discovered which could affect the content, and all legal disclaimers that apply to the journal pertain.

Keywords

Mammary Gland; Myoepithelial; Connexin; Gap Junctions; Contraction; Lactation

Introduction

Intercellular communication is essential for maintaining tissue- and organ-specific functions, and loss of cell-cell interaction is a hallmark of transformation and cancer (1). Gap junctions (GJs) are specialized conduits that couple cells electrically and metabolically, and regulate the selective passage of molecules of up to 1 kDa in size between the cytoplasm of adjacent cells (2–4). In vertebrates GJs are formed mostly by the connexin (Cx) family of proteins; six Cxs oligomerize to form a connexon hemichannel, and two connexons dock together joining the membranes of neighboring cells to form GJs. In mammals, connexins are encoded by at least 20 genes, which exhibit tissue- and cell-type-specific but overlapping patterns of expression (5, 6). Identical or different Cxs can oligomerize to form homomeric or heteromeric connexons respectively and the docking connexons in turn make homotypic or heterotypic GJs. The identity and stoichiometry of Cx distribution within GJs determines the permeability and gating properties of the channel, thus, regulating the type and rate of molecules passing between cells. The tissue context dictates Cx expression and in turn, distinct gap junctional channels maintain tissue-specific function (7, 8).

The mammary gland is a unique organ that develops mostly post-natally. An epithelial ductal rudiment is present at birth, which branches and elongates during puberty under the action of ovarian hormones to fill the mammary fat pad. The tree-like epithelial network is made of a bilayer of luminal duct lining and luminal milk secreting cells, surrounded by myoepithelial cells (myoeps) (9). Myoeps provide structural and functional support for their luminal counterparts and are contraction-competent (10). During pregnancy the alveolar compartment proliferates and expands to prepare for the ultimate function of lactation, during which alveolar luminal epithelial cells (leps) synthesize copious amounts of milk proteins. Systematic contraction of myoeps in response to suckling-mediated release of oxytocin facilitates the ejection of milk from the alveoli into the ducts en route to the nipple. For the past decade, the role of the myoepithelial compartment in the development and differentiation of the mammary gland has been gaining increasing attention (10–13). A growing body of evidence suggests that perturbation of the normal expression pattern of molecules specific to the myoepithelium alters the growth and differentiation of the entire gland. This is not surprising, since the mammary myoeps, with their physical location in the gland, are able to integrate multiple signals from neighboring cells and the underlying basement membrane (BM), and in turn, relay these signals to the luminal compartment to control cell growth, differentiation, and to maintain mammary architecture. Myoeps directly mediate the polarity of the mammary alveolar structures by secreting the BM protein Laminin 111. In fact, when leps are cultured in 3D collagen-I alone, they form “inside-out” acinar structures with inverted polarity, however, co-culturing normal mammary myoeps with leps in 3D collagen-I gels enables acinar formation with correct apico-basal polarity. This effect is inhibited when myoeps lacking laminin 111 are used in lep/myoep co-cultures, demonstrating the importance of myoeps in the secretion of laminin 111, and structural

organization of mammary acinar structures (13). In a different study (14), desmosomal cadherin-mediated interactions between leps and myoeps were shown to be essential for cellular positioning and tissue morphogenesis in 3D cultures of mammary epithelial cells, further highlighting the importance of lep/myoep interactions in regulating functional differentiation within the gland. (13, 14)

GJs were first described in the mammary gland in the work of Pitelka (1973) following visualization of the channels with freeze fracture and electron microscopy (15). Four Cxs have since been identified in the rodent mammary epithelium; Cx26, Cx30, and Cx32 are expressed in leps, whereas Cx43 is the only isoform expressed in the myoepithelium (16–18). The expression of all four subtypes in the mammary epithelium is temporally regulated and highest during late pregnancy and lactation, suggesting that connexins are important for functional differentiation of the gland. Cx26 and Cx32 are the dominant luminal isoforms expressed in the lactating mouse mammary epithelium; Cx26 levels are low in the mammary glands of nulliparous mice, but its levels increase as of early pregnancy and peak at parturition and lactation (19–22). Freeze-fracture and differential centrifugation studies showed that Cx32 and Cx26 can organize as either homomeric or heteromeric connexons and localize to the same junctional plaques. The stoichiometry of their association is regulated during lactation such that Cx32-Cx32 GJs replace Cx32-Cx26 GJs, as the latter are sensitive to and inhibited by the accumulation of taurine during this stage (18, 23, 24). Interestingly, the myoep Cx43 was shown to be hyper-phosphorylated at parturition (25). Previous studies have reported that Cx43 is important for the differentiation and contractile activity of smooth muscle cells (26). GJs made of Cx43 have been shown to account for the increased electrical coupling in the uterine myometrium, and a mouse with a smooth-muscle specific deletion of Cx43 exhibited delayed and defective parturition, implying a role of Cx43 in contraction of myometrial cells (27). A number of transgenic and knock-in mouse models of Cxs have shed better light on the specific and shared functions of the different Cx isotypes. Knock-in mice where the coding region for Cx43 was replaced by those of other Cxs (Cx26, Cx32 and Cx40) have been generated and described: whereas Cx40 was able to functionally substitute for Cx43 in the mammary gland, neither Cx26 nor Cx32 were able to fulfill Cx43 functions (8). Replacement of one copy of Cx43 by Cx26 altered the growth and differentiation of the mammary glands of Cx43^{43/26} knock-in female mice (28). In contrast, replacement of Cx43 by Cx32 led to compromised lactation in the glands of Cx43^{32/32} female mice, despite normal development of the glands (8). No lactation defects were observed in heterozygous Cx43^{+/-} mice, suggesting that the mammary phenotypes in the knock-in models are not only due to decreased levels of Cx43 but to a dominant-negative effect of the substituting Cxs. Similarly to the Cx43^{43/26} knock-in mice, transgenic mice expressing a mutant Cx43 (GJa1^{Jrt+/-}), showed impaired mammary gland growth and defective alveolar development, leading to ineffective milk synthesis and delivery to the newborns (29). Recent findings reveal that a critical level of Cx43-containing GJs is required, and below which, mammary function is impaired (30). As such, loss-of-function mutations in Cx43 that cause a partial decrease in GJ conductivity have milder mammary phenotypes. The variable outcomes of Cx loss and the limited functional overlap between Cx subtypes confirm the importance of tissue- and cell-specific expression of Cxs in maintaining tissue integrity.

Using a transgenic mouse model originally designed to study Cx26 overexpression in the skin, where the expression of Cx26 is driven by the Cytokeratin 5 (K5) promoter (31), we show here that targeting Cx26 expression to K5-expressing cells, impairs mammary function by inhibiting milk delivery to the pups. K5-driven Cx26 expression in transgenic mice (Tg) targets Cx26 to basal cells, and ectopically overexpresses Cx26 levels in myoeps. This leads to a concomitant decrease in endogenous Cx43, which disrupts GJ coupling between cells and causes a defect in myoep contraction. This is the first report of a trans-dominant negative interaction between Cx26 and Cx43 *in vivo*, validating our hypothesis that segregated expression and localization of GJ proteins provides the correct cues for functional integrity in the mammary gland.

Results

Failure of K5-Cx26 mothers to deliver milk at parturition leads to the demise of newborns

Although K5-Cx26 mice were designed to study the role of Cx26 in the skin (31), an unexpected problem arose while breeding the mice: pups born to K5-Cx26 transgenic (Tg) females were dying within few days after birth despite normal nursing behavior of their mothers. To determine if the failure to thrive was due to an abnormality with the pups or to a defect in lactation performance of the Tg dams, we prepared wild-type (WT) foster mothers and found that when litters born to Tg mothers were nursed by WT dams, the pups were healthy, and survived to weaning age (Fig. 1A). This suggested that the death of the pups was due to impaired lactational function in the mammary gland of Tg mothers. To investigate the cause of the mammary gland defect, we first looked at the localization of Cx26 to in the mammary glands of K5-Cx26 mice. K5 is a protein expressed in the glandular epithelial cells and myoeps of the mammary gland (12, 32, 33). Increased expression of K5 is observed in myoeps *in vivo*, and in cultured mammary epithelial cells. To determine whether Cx26 overexpression is targeted to the leps or myoeps in the mammary glands of Tg mice, we assessed Cx26 transcript and protein levels and its localization. Cx26 was mostly localized on the basal side of the mammary alveoli of Tg females, suggesting myoepithelial expression of the transgene (Fig. 1B and C). We demonstrated that Cx26 co-localizes with the myoep-specific smooth muscle alpha actin (SMA) protein in tissue sections of early lactating mammary glands, and in cultured cells derived from Tg but not WT females (Fig. S1). These data suggest that Cx26 overexpression via the K5 promoter targets the transgene ectopically to the myoeps, without significantly altering the expression of Cx26 in leps. Expectedly, Cx26 transcript levels were higher in Tg mammary glands across all developmental stages (Fig. 1D), whereas the expression of other mammary Cxs (Cx30, Cx32 and Cx43) was comparable in WT and Tg littermates (Fig. 1E). Similarly, Cx26 protein levels were higher in the glands of Tg mice across all developmental stages (Fig. 1F). We sought to determine how targeting of Cx26 to the myoepithelial layer interferes with lactational performance in K5-Cx26 mothers. Upon examination of the newborns, we observed a lack of milk spots in their abdomen by the first two days post-parturition, despite repetitive nursing attempts by the mothers (Fig. 2A). We thus asked whether the inability of the K5-Cx26 females to feed their litters at parturition is caused by insufficient milk production. We analyzed milk gene expression and protein levels and showed that tissues from mid-pregnant (day 14), late-pregnant (day 18) and early

Author Manuscript

Author Manuscript

Author Manuscript

lactating (day 1) WT and Tg littermates have comparable expression of β -casein and whey acidic protein (WAP) as well as similar β -casein protein levels (Fig. 2B). Interestingly, the mammary glands of Tg mice were engorged and distended in the two days post parturition compared to those of WT littermates, suggesting that milk was accumulating in the gland (data not shown). By day 10 post-parturition, β -casein levels were lower in the mammary glands of Tg mothers, reflecting early involution of the gland caused by milk stasis. This is not surprising, since the cessation of suckling after the demise of the litter leads to milk accumulation, signaling for the start of involution. Examining whole mount and histological sections of the mammary glands from WT and Tg mice revealed that age-matched nulliparous, pregnant, and lactating littermates have comparable ductal or alveolar growth and size, suggesting that mammary glands of Tg mice develop normally (Fig. 2C). Morphometric analysis confirmed that the epithelial to stromal ratios are similar in the mammary glands of WT and Tg littermates in pregnancy and early lactation, suggesting that the glands of Tg females undergo normal alveolar growth and expansion. In contrast, by day 10 of lactation, the number of epithelial to stromal cells in the glands of Tg females is significantly lower compared to their WT littermates, similarly to the observed decrease in milk protein levels, and reflecting the early onset of involution (Fig. 2D). We thus concluded that the premature death of pups born to Tg mothers was not due to mammary developmental effects affecting milk production, and we sought other explanations for the inability of K5-Cx26 mothers to deliver milk to the newborns.

Impaired milk delivery by K5-Cx26 mothers is caused by a defective contractile apparatus in the K5-Cx26 alveoli

Author Manuscript

Author Manuscript

Mammary myoeps contract in response to suckling-mediated release of oxytocin after parturition. We assessed the response of the mammary glands from WT and Tg dams to the addition of exogenous oxytocin *ex vivo*. Mammary glands of freshly euthanized WT and Tg animals were supplied with oxytocin as described previously (26, 29) and the release of milk into the major ducts was documented by imaging after oxytocin addition. Exogenous addition of oxytocin, but not PBS, induced a visible release of milk into the large ducts leading toward the nipples around 10 minutes after the addition of the hormone in WT mice. In contrast, oxytocin addition to glands of Tg females did not lead to milk release into the ductal system (Fig. 3A). Thus, we hypothesized that the Tg dams have a milk ejection defect, possibly due to impaired contraction of the myoeps. To test our hypothesis we developed a culture assay based on our 3D organotypic culture system (Fig. 3B). We cultured primary organoids isolated from the glands of WT and Tg littermates on top of IrECM gels, and supplied them with lactogenic hormones for 4 days. After 4 days, we added either PBS vehicle, or oxytocin (OT) to the primary organoids and immediately visualized them under live microscopy for 40 minutes to 2 hours after OT addition (Fig. 3C). Whereas, organoids from WT female mice pulsed and contracted after OT addition (supplemental movies 1A, B, C), organoids from Tg mice did not contract in response to OT addition (supplemental movies 2A, B, C). Interestingly, impairment of contraction occurred despite normal levels of oxytocin receptors (OTR) in the glands of Tg mice (Fig. 3D), suggesting that the defect is downstream from oxytocin receptor activation.

Myoepithelial differentiation and oxytocin receptor signal transduction are similar in organoids from Tg and WT mice

The failed response to oxytocin in the mammary glands of Tg females could be due to one of three possibilities: 1) an insufficient number of myoeps in the glands of Tg females, due to defective epithelial lineage determination, 2) an impairment in the differentiation of myoeps in the glands of adult Tg mice, or 3) a defect in the intracellular signaling pathways downstream from oxytocin receptors. We had investigated the possibility of lower numbers of myoeps in the glands of Tg mice by using FACS-mediated analysis of the lep and myoep fractions in the glands of WT and Tg females. Fractionation of the two cell types from the glands of WT and Tg females revealed no significant differences in the ratios of mammary myoeps to leps between WT and Tg animals (Fig. S2), suggesting that glands of Tg females have adequate numbers of myoeps to enable contraction. We then assessed whether the myoeps in Tg glands are fully differentiated by examining the levels of smooth muscle- and myoep- specific proteins from WT and Tg mice, using either isolated myoeps, or whole tissue lysates. The levels of alpha-smooth muscle actin (SMA) or Keratin 14 or p63 were similar between the WT and Tg littermates (Fig. 4A, a, b), suggesting that myoeps from Tg females differentiate to acquire smooth-muscle characteristics. We then investigated the intracellular signaling pathway in response to oxytocin stimulation. Previous studies have shown that phosphorylation of myosin light chain2 (MLC2) is required for smooth muscle contraction, and that a balance between pMLC2 and MLC2 levels allows the completion of a contraction/relaxation cycle in smooth muscle cells (34). To determine if signaling from oxytocin to the contractile machinery was compromised in the glands of Tg females, we first assessed the levels of pMLC2 to MLC2: Western blot analysis revealed that pMLC2 levels are comparable in the glands of WT and Tg females during the first day of lactation (Fig. 4B). Since our previous results revealed that pulsing in response to oxytocin occurs at ~20 min after addition of the hormone to primary mammary organoids, we assessed the levels of phosphorylated MLC2 upon addition of oxytocin to WT and Tg organoids in culture. Addition of the hormone, caused comparable phosphorylation of MLC2 in primary organoids isolated from WT and Tg littermates, confirming adequate activation of the intercellular signaling cascade in Tg cells upon oxytocin administration (Fig. 4C). The experiment was repeated 3 times with slight variations within each genotype; however densitometric analysis revealed that the differences were not significant or genotype-specific (Fig. 4C). These data suggest that myoeps from Tg females respond to oxytocin biochemically, but may not be able to respond mechanically, despite normal levels of smooth muscle proteins. We thus asked what could inhibit the fulfillment of a contractile response in the organoids of Tg females?

Ectopic expression of Cx26 acts as a trans-dominant negative for Cx43 protein function

In addition to biochemical signaling from the oxytocin receptor, successful contraction requires synchronized depolarization waves, which are dependent on effective gap junctional communication. In myoepithelial cells, Cx43 is the endogenous gap junction protein required for normal myoep-myoep communication, and loss of Cx43 in other contractile tissue has been shown to inhibit contraction (26). Although Cx43 transcript levels were unaltered in the glands of K5-Cx26 mice, Western analysis revealed that Cx43 protein and phosphorylation levels are significantly lower in the glands of Tg females (Fig. 5A and B).

Immunostaining correlated with the western blot data showing decreased signal for Cx43 in the Tg mammary gland (Fig. S3). These unexpected findings suggested that ectopic expression of Cx26 affects the protein levels, post-translational modification, and stability of Cx43. Interestingly only Cx43 was affected by the overexpression of Cx26 as protein levels of Cx30 and Cx32 were comparable in the mammary glands of WT and Tg littermates in late pregnancy and early lactation (Fig. 5C). These data suggest that Cx26 acts as a trans-dominant negative to Cx43 in Tg myoeps. We thus asked if Cx43 loss impairs gap junctional communication in the myoeps of Tg mice, and whether decreased gap junctional coupling is the cause of the contraction defect in K5-Cx26 females.

Loss of Cx43-mediated gap junctional communication leads to defective myoepithelial contraction

To determine whether loss of gap junctional communication was responsible for the contraction defect seen in the mammary glands of the K5-Cx26 dams, we assessed the response of primary WT organoids in culture to the addition of oxytocin in the presence of a gap junction inhibitor, 18 α -glycerritinic acid (18 α GA). WT organoids were treated with 10 and 50 μ M 18 α GA before addition of oxytocin. Inhibition of gap junctional communication in organoids isolated from WT animals recapitulated the contraction defect observed in Tg organoids suggesting that the loss of communication was sufficient to cause a contraction defect in response to oxytocin administration (Fig. 6A and supplemental movies 3A&B, 4A&B, 5A&B). Knock down of Cx43 in WT mammary organoids using shRNA interference resulted in defective contractile response to oxytocin, suggesting that Cx43 loss alone was sufficient to impair contraction of the myoeps in the organoid cultures (Fig. 6B and supplemental movies 6A&B, 7A&B). Because inhibition of gap junctional communication or the specific loss of Cx43 impaired oxytocin-mediated contraction of WT primary organoids, we hypothesized that Cx43 loss in the glands of Tg mice, alters gap junctional communication, causes defective contraction by impairing gap junctional communication. Using a standard scrape loading assay (35) on primary mammary cells isolated from WT and Tg animals, followed by staining with anti-Cx26 antibodies, we observed that in the primary cultures from Tg females, cells highly expressing Cx26 are impermeable to standard LY dye. This finding suggests that myoeps expressing high levels of Cx26 are unable to appropriately communicate via gap junctions, consistent with the loss of the endogenous Cx43 (Fig. 7). We conclude that the mammary phenotype of the K5-Cx26 is the result of Cx26 acting as a trans dominant negative to Cx43 function, which results in dysfunctional communication through GJs, leading to a contractile defect in the mammary glands of Tg mice.

Discussion

The importance of gap junctional communication in normal mammary function is uncontested (19, 20). In the rodent mammary gland, Cx distribution is asymmetric, with Cx26, Cx30, Cx32 expressed in the luminal epithelium and Cx43 in the myoeps (16, 18). Although many tissues express two or more members of the Cx family and that two Cxs can be co-expressed in the same cell, there is little functional overlap between Cx subtypes. The need for molecular heterogeneity of Cxs is not surprising: Cx-pairing specificity within gap

junctions dictates which cell types are able to communicate with each other, and modulates the type and rate of molecules passing through gap junctions (6, 36).

In this study we revealed the consequences of mis-expressing a luminal Cx in the myoepithelium. Using a K5-Cx26 transgenic mouse, we found that mammary glands of K5-Cx26 female mice develop normally but the transgenic females are unable to feed their pups, leading to litter starvation and demise of the pups during the stages of early to mid-lactation. Furthermore we determined that the inability to feed the pups is caused by impaired milk delivery, despite normal mammary alveolar development and milk protein expression. Surprisingly, we found that ectopic expression of Cx26 in myoepithelial cells alters the expression of endogenous Cx43. The decrease in Cx43 protein levels caused by overexpression of Cx26 leads to inhibition of gap junction-mediated communication as observed by loss of dye coupling in cells expressing high levels of Cx26.

Other studies have also demonstrated the importance of cell- and tissue- specific Cx distribution. For example, replacement of one copy of Cx43 by Cx26 in the mammary glands of a knock-in mouse (Cx43^{43/26}) impacts mammary function (28). Although both K5-Cx26 and Cx43^{43/26} express Cx26 in the myoeps, their mammary phenotypes are different: whereas glands of K5-Cx26 females develop normally but have a contraction defect after parturition, the mammary glands of Cx43^{43/26} females have developmental defects from earlier stages. Similarly, transgenic mice expressing a mutant Cx43 (GJa1^{Jrt+/-}), have impaired mammary gland growth and development, leading to litter starvation after parturition. In contrast, heterozygous Cx43^{+/-} mice have no mammary defects, suggesting that decreased levels of WT Cx43 alone are not sufficient to disrupt mammary development, but a novel study has shown that there is a critical level of Cx43 that is required for normal mammary function, and different mutations in *Gja1*, that result in variable levels of Cx43 expression cause different phenotypes (30). Surprisingly, Cx43^{32/32} mice, where both copies of Cx43 are replaced by Cx32, have a comparable mammary phenotype to K5-Cx26 mice, whereby mothers are unable to feed their pups despite normal mammary gland development (8, 37). These findings highlight the subtle and intricate variations in the shared and unique functions of the different Cxs, and underscore the importance of spatio-temporal control over Cx expression.

It has been suggested, and supported by our findings, that Cx43 is essential for oxytocin-mediated myoepithelial contraction in the mammary gland. In fact, loss of Cx43 affects smooth muscle contractility in other oxytocin-responsive tissues, such as the uterine myometrium. In particular, either the specific ablation of Cx43 in smooth muscle cells, or the expression of a mutant Cx43 in the uterine myometrium caused delayed parturition and the birth of suffocated pups (26, 27). Delayed and defective parturition were attributed to decreased contractions in myometrial smooth muscle cells, and the contractile impairment correlated with lower gap junctional communication between myometrial cells compared to wild type counterparts (26, 27).

Only Cx26 and Cx43 are expressed in the human breast, and predominantly exhibit a segregated pattern of expression between luminal and myoepithelial cells, although some studies suggest that Cx43 is expressed in luminal breast cells as well (38, 39). The

developmental patterns of Cx expression in the human breast is difficult to study, owing to the inability to obtain tissue biopsies at distinct stages. As such, most data on Cx expression in the human breast are either from reduction mammoplasties, or from cancer patients. Multiple studies have shown decreased levels of both Cx26 and Cx43 in breast cancer biopsies, and some have even suggested that restoration of Cx expression can attenuate the invasive/tumorigenic phenotype (40, 41). However, other studies showed that Cx expression is increased in a variety of cancers, particularly at sites of metastasis (42–44). Although there are no known diseases where Cx26 is ectopically expressed in breast myoeps, there are many diseases that are caused by mutations in Cx26 gene (GJB2) and Cx43 (GJA1). GJB2 mutations are responsible for a host of syndromic and non-syndromic diseases including hereditary deafness and hyper-keratosis. Patients with Cx26-associated diseases report a variety of phenotypes either caused by loss-of-function or gain-of-function mutations, however, there are no known reports about lactation problems in these patient populations (45–47). In this mouse model, Cx26 expression by the K5 promoter targeted Cx26 to Cx43-expressing basal keratinocytes in the skin, where Cx26 expression was previously shown to be highly and transiently induced during pathologic conditions such as wound healing, psoriasis, and skin hyperplasia and carcinogenesis. Interestingly, ectopic expression of Cx26 did not affect Cx43 levels in keratinocytes, nor did it lead to increased proliferation of basal keratinocytes as expected; on the contrary, it reduced proliferation, especially in response to the tumor promoter TPA (31). We did not assess whether K5Cx26 mice had increased susceptibilities to developing mammary tumors.

Ours is the first report of a dominant-negative interaction between WT Cx26 and Cx43 *in vivo*. We showed that Cx43 mRNA expression is not affected by the ectopic expression of Cx26, but that Cx43 protein levels and phosphorylation are significantly lower in Tg mice compared to WT littermates. Interestingly, Cx26 and Cx43 are co-expressed in many tissues and in cultured cells, but to date they have not been shown to assemble into heteromeric hemi-channels. Cx26 and Cx43 proteins are structurally distinct, and, whereas Cx43 has multiple phosphorylation sites, Cx26 is unphosphorylated and has a significantly shorter carboxy-terminal tail compared to the other Cx subtypes, and particularly relative to Cx43 (48). Different studies have revealed variable routes of shuttling of Cx26 and Cx43 to the membrane, and most studies argue that segregated routing of the proteins impedes their oligomerization and assembly at the membrane. (49–55). Another striking feature of these two Cx isotypes is that their co-expression in the same cell was shown to reduce the total intercellular junctional conductance to a little more than 10% of that in cells expressing only a single Cx (either Cx26 alone or Cx43 alone) (52). This could be due to the presence of incompatible connexons at the apposing membranes, or the presence of competitive connexons within the cell, which recruit gating regulators away from the nearby channels, both ultimately resulting in decreased overall connectivity. It is possible that Cx26 is able to reach the membrane in K5-Cx26 myoeps but that channels remain closed, or that they are impermeable for specific molecules that are important for electrical conductance and the spread of the depolarization wave during oxytocin-mediated contraction. We have not determined how Cx26 causes down-regulation of Cx43 protein in the mammary myoeps of K5-Cx26 mice, but our findings emphasize the importance of segregated distribution of gap

junction proteins in the mammary gland, and further highlight the important role of Cx43 and gap junctional communication in contractile function of mammary myoeps.

Materials and Methods

Animals and Tissue Collection

Engineering of K5-Cx26 transgenic mice was described previously (31). Two K5.Cx26 mouse lines were used; line 73 and line 75, and both were maintained in the same FVB background. In all experiments the age-matched wild type littermates were used as control. K5-Cx26 males were crossed with wild-type (WT) females to generate an F1 progeny with transgene positive females (Tg) and WT littermate controls. All animals were cared for in accordance with the Lawrence Berkeley National Laboratory Animal Welfare Regulatory Committee. Identification of transgenic mice was done by PCR analysis of tail DNA using vector specific primers (5'-TTC AGG GTG TTG TTA GAA TGG-3' and 3'-CAA TAA GAA TAT TTC CAC GCC A -5'). Mammary gland tissue was collected as previously described (56): the thoracic 2nd and 3rd mammary glands and inguinal 4th mammary glands were excised and either snap frozen on dry ice for RNA, DNA, and protein isolation, or whole mounted for morphologic analysis, or formalin fixed and paraffin embedded for histologic analysis. For whole-mount analysis, one 4th inguinal mammary gland from each mouse was spread onto a glass slide, immersed in Carnoy's fixative overnight, stained with carmine alum, and de-stained with acidic alcohol.

Primary organoid culture

The thoracic 2nd and 3rd mammary glands and 4th inguinal mammary glands were removed from mice. Minced tissue (4–8 glands) was gently shaken for 30 min at 37 °C in a 50-ml collagenase/trypsin mixture (0.2% trypsin, 0.2% collagenase type IV, 5% fetal calf serum, 5 µg/ml Insulin, 50 µg/ml gentamycin, in 50 ml of DMEM/F12). The collagenase solution was discarded after centrifugation at 1000 rpm and the pellet was re-suspended in 10 ml DMEM/F12. The suspension was pelleted again at 1000 rpm for 10 min, re-suspended in 4 ml of DMEM/F12 + 40 µl of DNase (2 U/µl), and incubated for 5 min at ambient temperature with occasional shaking. The DNase solution was removed after centrifugation at 1000 rpm for 10 min. The DNase solution was discarded and the epithelial pieces were separated from the single cells through differential centrifugation. The pellet was re-suspended in 10 ml of DMEM/F12 and pulsed to 1500 rpm. The supernatant was then removed and the pellet was re-suspended in 10 ml DMEM/F12. Differential centrifugation was performed at least 4 times. The final pellet was re-suspended in the desired amount of basal medium (DMEM/F12 with 1% insulin, transferrin, selenium, and 1% penicillin/streptomycin) and seeded on top of a thin layer of Matrigel™ (Growth Factor Reduced Matrigel, BD Biosciences, San Jose, CA) for 24 h. After 24 h, the media was either replenished or changed to differentiation medium with lactogenic hormones: 1 µg/ml hydrocortisone (Sigma-Aldrich; GIH medium) and 1 µg/ml sheep Prl (Sigma-Aldrich), and dripped with 15% lrECM (Matrigel™).

Fractionation of mouse mammary epithelial cell types

To fractionate the epithelial subtypes from each other (i.e. the luminal epithelial cells and myoeps from each other) isolated primary mammary organoids were re-suspend in Joklik's Ca-free medium at 37°C for 15 min, then centrifuged at 1500 rpm for 10 min at room temperature and re-suspend them in 2 mL of Hank's Balanced Salt Solution at 37°C for 5 min. The organoids were then incubated with 5 mL of serum-free DMEM/F12 with type-I DNase (50 μ L of 2U/mL DNase I) to remove clumps and the reaction was stopped with 10% FBS in 5mL of L-15 medium or in calcium free DMEM/F12 with DNAase (50 μ L, 2U/mL). The cells were then collected and washed and passed through a pre-separation filter and re-suspended in 500 μ L FACS buffer (2.5% Fetal Bovine Serum in 1X PBS) for fluorescence activated cell sorting. AlexaFluor 647-anti mouse EpCAM, and FITC anti-mouse CD104 (BioLegend®) were used for labelling of leps and myoeps respectively, before FACS.

Protein Extraction and Western Blot Analysis

Mammary glands were homogenized in 500 μ L of lysis buffer (50 mM Tris-Cl, pH 7.5, 150 mM NaCl, 1% Nonidet P40, 0.5% sodium deoxycholate, phosphatase inhibitor cocktail of NaF (1 mM) and Na₃VO₄ (1.25 mM) and protease inhibitor cocktail from Calbiochem, EMD Biosciences, San Diego, CA). Protease inhibitors were added at a concentration of 40 μ L/1 ml of lysis buffer, and phosphatase inhibitors cocktail at a concentration of 10 μ L/1 ml each. The homogenate was centrifuged at 12,000 $\times g$ for 20 minutes at 4°C. For protein isolation from primary organoids, medium was removed from the well, and Matrigel + organoids were washed once with cold 1 \times PBS containing NaF (1 mM) and Na₃VO₄ (1.25 mM) and incubated with Matrigel extraction buffer (1 \times PBS containing NaF (1 mM) and Na₃VO₄ (1.25 mM) 5mM EDTA) on ice for 30 minutes with shaking to remove residual Matrigel, then protein extraction from organoids proceeded as described above for whole mammary glands.

The protein concentrations of supernatants were determined by Bio-Rad detergent-compatible protein assay (Bio-Rad Laboratories, Hercules, CA).

Mammary protein (10 μ g) was loaded onto 4–20% Tris-glycine gels for SDS-PAGE. Transfer efficiency was determined by Ponceau S staining and equal loading was confirmed by Lamin A/C levels (Santa Cruz Biotechnology, inc.).

Membranes were blocked for one hour in wash buffer (1 \times TBST: 100 mM Tris-HCl buffer, pH 7.5, 150 mM NaCl, 0.1–0.3% Tween 20) with 5% milk for Cx proteins or 5% bovine serum albumin for milk proteins. Primary antibody was diluted in blocking buffer and the membranes were incubated overnight at 4°C in: polyclonal rabbit anti-mouse milk serum (Bissell laboratory) diluted 1:10,000 in blocking buffer, with polyclonal rabbit anti-Cx26 (Invitrogen Cat#51-2800) or monoclonal mouse anti-Cx26 (Invitrogen Cat#33-5800), and polyclonal rabbit anti-Cx43 (Invitrogen Cat# 71-0700), polyclonal rabbit anti-catenin peptide (Santa Cruz biotechnology, inc. Cat# sc-7894 for α -catenin, Cat# sc-7199 for β -catenin) at a concentration of 0.5 μ g/ml in blocking buffer, and, with rabbit anti-myosin light chain 2 and anti-phospho-myosin light chain 2 (Cell signaling Car#3672, 3674) at a dilution of 1:200 on blocking buffer, rabbit anti-alpha smooth muscle actin (abcam, Cat#ab5694),

rabbit anti-p63 (abcam, Cat#ab53039), rabbit anti-keratin 5 (Covance, Cat#PRB-160P) at a dilution of 1:500 in blocking buffer.

Membranes were then washed three times, for 10 min each and incubated with horse raddish peroxidase-conjugated secondary antibodies in 5% 1× TBST for 1 hour at room temperature. Chemiluminescent detection of bands was achieved using Pierce SuperSignal West Femto Maximum Sensitivity Substrate (Pierce, Rockford, IL).

RT-PCR

Total RNA was isolated with QIAGEN RNeasy Mini Kit (Valencia, CA). For cDNA synthesis, 20 ng of total cellular RNA was used to synthesize cDNA using SuperScript III First-Strand Synthesis System (Invitrogen, Carlsbad, CA). Primers for Cx26, Cx30, Cx32, Cx43, β -casein and whey acidic protein were used. Cx26 (sense: gaatgtatgctacgaccacca, antisense: ctttcctgagcaatacctaag); Cx30 (sense: ggggtaccacctacctgggtac, antisense: tgcattctggcactatctgag); Cx32 (sense: aatgctacggcttgaggggcatg, antisense: gcctgctcaccggcataggag); Cx43 (sense: gttcagcctgagtgccgtctac, antisense: ggctctgctggaagtcgctgac); β -casein (sense: gtggcccttgctcttgaag, antisense: agtctgagaaaaagcctaag); WAP (sense: atcgcttgccctcagcc, antisense: gacagccagggatggc). Real-time PCR was performed using LightCycler System (Roche Diagnostics, Indianapolis, IN) according to the manufacturer's instructions. Fast Start DNA Master SYBR Green I (Roche Diagnostics, Indianapolis, IN) was used for PCR reaction. PCR data were analyzed with LightCycler Software ver.3 (Roche Diagnostics, Indianapolis, IN). Relative signals between Cxs and 18s rRNA were quantified.

Immunocytochemistry and Confocal Microscopy

Mammary gland cryosections (thickness, 5 μ m) and cells were fixed in 10% buffered formalin and 80% methanol/20% acetone before immunolabeling with primary antibodies: rabbit anti-Cx26 (1 μ g/ml), rabbit anti-Cx30 (1.25 μ g/ml), rabbit anti-Cx32 (10 μ g/ml), rat anti-E-cadherin (2.5 μ g/ml), rabbit anti- β -catenin (2.5 μ g/ml), rabbit anti-keratin 5 antibody (2 μ g/ml; all from NeoMarkers), FITC anti-alpha smooth muscle (Sigma). Cryosections and cells were then immunolabeled with secondary antibodies. DAPI staining was used to visualize nuclei before mounting with ProLong antifade (Invitrogen). Paraffin-embedded sections were subjected to rehydration with descending grades of ethanol baths to 1XPBS. Antigen retrieval was done by microwaving samples on high for 40 minutes in sodium citrate buffer (pH 6). Sections were then permeabilized and blocked with 0.1% Triton X-100 and 5% bovine serum albumin in PBS for 60 min and incubated with antibodies. Primary antibody was visualized by incubating sections with Alexafluor dye-conjugated secondary antibodies. DAPI stain was used to visualize nuclei before mounting with ProLong antifade (Invitrogen). Immunolabeled cryosections and paraffin-embedded sections were imaged on a Zeiss LSM 710 confocal microscope, and images were exported using Zen 2009 software and ImageJ for display.

Whole mounting and Histology

To perform a general histological analysis of the mammary gland, paraffin-embedded sections of WT and K5-Cx26 mammary glands were stained with hematoxylin and eosin.

Paraffin-embedded mammary gland sections were deparaffinized in xylene for 10 min, rehydrated in descending grades of ethanol baths, and stained with 1% hematoxylin (5 min) and 1% eosin (5 min). Sections were dehydrated in ascending grades of ethanol and xylene baths and mounted with Cytoseal (Richard-Allan Scientific). General histological analysis was performed by imaging several random areas with 63×, 40×, and 16× objective lenses mounted on a Zeiss Axioscope microscope workstation equipped with a Sony PowerHAD camera and Axiovision LE imaging software (Carl Zeiss Vision).

Oxytocin induced assays

Ex vivo oxytocin assay was done as previously described (29). Pups were removed from the dam 1 h prior to the assay and the mouse was sacrificed on parturition day. Abdominal skin was cut and peeled off in order to expose the mammary gland. PBS or 0.5µg/ml–1 mg/ml oxytocin in PBS was applied directly on the mammary glands for 1 min and then removed. Milk entry into the ducts was monitored using a numeric camera. Photographs were taken before and after PBS or oxytocin exposure.

To visualize contraction in culture, primary organoids were seeded on top of a layer of Matrigel™ and supplied with lactogenic hormones (for 4 days to induce the production of milk proteins. After 4 days, organoids were subjected to oxytocin (10^{-6} i.u/ml) (Sigma) and tracked by live imaging for different lengths of time; serial images were obtained at rates of 1 frame per every 0.05 seconds for the individually imaged organoids, or 1 frame every 2 minutes for longer time periods and a wider image area. Live imaging was done on an LSM 710 microscope. Images were later processed either on the LSM 710 ZEN Light edition software, or using ImageJ. Quantification of contractility was done using ImageJ software. Briefly, serial images of organoids were imported into ImageJ as stacks and single organoids were selected for each analysis. Selected organoid stacks were binarized to enable analysis, and background noise was reduced using ImageJ built-in noise reduction functions. Binary images were processed using the “Analyze Particles” feature to measure the change of surface area in the successive image stacks. The results displaying the surface area of organoids for each acquired image/frame, were copied to Microsoft Excel, where the change of surface area (δ) for each time point, compared to the original measurement was calculated as a Relative Area Change as follows:

$$\text{Relative Surface Area Change}_{(Tx)}: \delta A_{(Tx)} = (A_{Tx} - A_{T0}) / A_{T0}$$

The change in Surface Area was then plotted over time for randomly selected organoids (supplemental excel files 1–4).

Cx43 Knockdown

shRNA constructs (in pLKO.1-puro plasmids) selectively targeting Cx43 (GJA1) were purchased from MISSION shRNA library (Sigma). Control cells were infected with nontargeting shRNA. Knockdown efficiency was verified by Western blotting with the appropriate antibodies.

shRNA #1	CCGGCCACCTTTGTGTCTCCATACTCGAGTATGGAAGACACAAAGGTGGGTTTTTG
shRNA #2	CCGGGCTCTCTATGTCTCTTCAACTCGAGTTGAAGAAGACATAGAAGAGCTTTTTG

For transduction, organoids were seeded in 12-well polyhema-coated plates (~2000 organoids per well) and infected with lentivirus in the presence of 8 µg/mL polybrene for 24 h and using MISSION ExpressMag Beads (Sigma) according to the manufacturer's instructions. Cells transduced with lentivirus carrying shRNA constructs were selected with 2 µg/mL puromycin.

Scrape Loading Assay

Primary cells were washed three times with warm PBS before addition of Lucifer yellow-CH (LY) at 0.1% dilution in PBS. Using a scalpel, cuts were made throughout the monolayer, followed by incubation with 5% LY in 150 mM LiCl for 10 min at 37 °C. The cells were then washed with warm PBS and fixed with 4% formaldehyde. Slides were preserved by mounting in anti-fade and stored at 4 °C for later analysis and quantification.

Supplementary Material

Refer to Web version on PubMed Central for supplementary material.

References

1. Sulkowski S, Sulkowska M, Skrzydlewska E. Gap junctional intercellular communication and carcinogenesis. *Pol J Pathol.* 1999; 50:227–233. [PubMed: 10721262]
2. Kumar NM, Gilula NB. The gap junction communication channel. *Cell.* 1996; 84:381–388. [PubMed: 8608591]
3. Maeda S, Tsukihara T. Structure of the gap junction channel and its implications for its biological functions. *Cell Mol Life Sci.* 2011; 68:1115–1129. [PubMed: 20960023]
4. Maeda S. Structure and function of human gap junction channel. *Tanpakushitsu Kakusan Koso.* 2009; 54:1760–1766. [PubMed: 19827609]
5. Sohl G, Willecke K. Gap junctions and the connexin protein family. *Cardiovasc Res.* 2004; 62:228–232. [PubMed: 15094343]
6. Mroue RM, El-Sabban ME, Talhouk RS. Connexins and the gap in context. *Integr Biol (Camb).* 2011; 3:255–266. [PubMed: 21437329]
7. Bevans CG, Kordel M, Rhee SK, Harris AL. Isoform composition of connexin channels determines selectivity among second messengers and uncharged molecules. *J Biol Chem.* 1998; 273:2808–2816. [PubMed: 9446589]
8. Plum A, Hallas G, Magin T, Dombrowski F, Hagendorff A, Schumacher B, Wolpert C, Kim J, Lamers WH, Evert M, Meda P, Traub O, Willecke K. Unique and shared functions of different connexins in mice. *Curr Biol.* 2000; 10:1083–1091. [PubMed: 10996788]
9. Richert MM, Schwertfeger KL, Ryder JW, Anderson SM. An atlas of mouse mammary gland development. *J Mammary Gland Biol Neoplasia.* 2000; 5:227–241. [PubMed: 11149575]
10. Adriance MC, Inman JL, Petersen OW, Bissell MJ. Myoepithelial cells: good fences make good neighbors. *Breast Cancer Res.* 2005; 7:190–197. [PubMed: 16168137]
11. Deugnier MA, Teuliere J, Faraldo MM, Thiery JP, Glukhova MA. The importance of being a myoepithelial cell. *Breast Cancer Res.* 2002; 4:224–230. [PubMed: 12473168]

12. Deugnier MA, Moiseyeva EP, Thiery JP, Glukhova M. Myoepithelial cell differentiation in the developing mammary gland: progressive acquisition of smooth muscle phenotype. *Dev Dyn.* 1995; 204:107–117. [PubMed: 8589435]
13. Gudjonsson T, Adriance MC, Sternlicht MD, Petersen OW, Bissell MJ. Myoepithelial cells: their origin and function in breast morphogenesis and neoplasia. *J Mammary Gland Biol Neoplasia.* 2005; 10:261–272. [PubMed: 16807805]
14. Runswick SK, O'Hare MJ, Jones L, Streuli CH, Garrod DR. Desmosomal adhesion regulates epithelial morphogenesis and cell positioning. *Nat Cell Biol.* 2001; 3:823–830. [PubMed: 11533662]
15. Pitelka DR, Hamamoto ST, Duafala JG, Nemanic MK. Cell contacts in the mouse mammary gland. I. Normal gland in postnatal development and the secretory cycle. *J Cell Biol.* 1973; 56:797–818. [PubMed: 4569313]
16. Talhouk RS, Elble RC, Bassam R, Daher M, Sfeir A, Mosleh LA, El-Khoury H, Hamoui S, Pauli BU, El-Sabban ME. Developmental expression patterns and regulation of connexins in the mouse mammary gland: expression of connexin30 in lactogenesis. *Cell Tissue Res.* 2005; 319:49–59. [PubMed: 15517403]
17. El-Sabban ME, Abi-Mosleh LF, Talhouk RS. Developmental regulation of gap junctions and their role in mammary epithelial cell differentiation. *J Mammary Gland Biol Neoplasia.* 2003; 8:463–473. [PubMed: 14985641]
18. Locke D, Stein T, Davies C, Morris J, Harris AL, Evans WH, Monaghan P, Gusterson B. Altered permeability and modulatory character of connexin channels during mammary gland development. *Exp Cell Res.* 2004; 298:643–660. [PubMed: 15265710]
19. Monaghan P, Perusinghe N, Carlile G, Evans WH. Rapid modulation of gap junction expression in mouse mammary gland during pregnancy, lactation, and involution. *J Histochem Cytochem.* 1994; 42:931–938. [PubMed: 8014476]
20. Monaghan P, Moss D. Connexin expression and gap junctions in the mammary gland. *Cell Biol Int.* 1996; 20:121–125. [PubMed: 8935156]
21. Tu ZJ, Pan W, Gong Z, Kiang DT. Involving AP-2 transcription factor in connexin 26 up-regulation during pregnancy and lactation. *Mol Reprod Dev.* 2001; 59:17–24. [PubMed: 11335942]
22. Tu ZJ, Kollander R, Kiang DT. Differential up-regulation of gap junction connexin 26 gene in mammary and uterine tissues: the role of Sp transcription factors. *Mol Endocrinol.* 1998; 12:1931–1938. [PubMed: 9849966]
23. Locke D, Koreen IV, Harris AL. Isoelectric points and post-translational modifications of connexin26 and connexin32. *FASEB J.* 2006; 20:1221–1223. [PubMed: 16645047]
24. Yamanaka I, Kuraoka A, Inai T, Ishibashi T, Shibata Y. Differential expression of major gap junction proteins, connexins 26 and 32, in rat mammary glands during pregnancy and lactation. *Histochem Cell Biol.* 2001; 115:277–284. [PubMed: 11405055]
25. Yamanaka I, Kuraoka A, Inai T, Ishibashi T, Shibata Y. Changes in the phosphorylation states of connexin43 in myoepithelial cells of lactating rat mammary glands. *Eur J Cell Biol.* 1997; 72:166–173. [PubMed: 9157013]
26. Tong D, Lu X, Wang HX, Plante I, Lui E, Laird DW, Bai D, Kidder GM. A dominant loss-of-function GJA1 (Cx43) mutant impairs parturition in the mouse. *Biol Reprod.* 2009; 80:1099–1106. [PubMed: 19176884]
27. Doring B, Shynlova O, Tsui P, Eckardt D, Janssen-Bienhold U, Hofmann F, Feil S, Feil R, Lye SJ, Willecke K. Ablation of connexin43 in uterine smooth muscle cells of the mouse causes delayed parturition. *J Cell Sci.* 2006; 119:1715–1722. [PubMed: 16595547]
28. Winterhager E, Pielensticker N, Freyer J, Ghanem A, Schrickel JW, Kim JS, Behr R, Grummer R, Maass K, Urschel S, Lewalter T, Tiemann K, Simoni M, Willecke K. Replacement of connexin43 by connexin26 in transgenic mice leads to dysfunctional reproductive organs and slowed ventricular conduction in the heart. *BMC Dev Biol.* 2007; 7:26. [PubMed: 17408477]
29. Plante I, Laird DW. Decreased levels of connexin43 result in impaired development of the mammary gland in a mouse model of oculodentodigital dysplasia. *Dev Biol.* 2008; 318:312–322. [PubMed: 18455714]

30. Stewart MK, Gong XQ, Barr KJ, Bai D, Fishman GI, Laird DW. The severity of mammary gland developmental defects is linked to the overall functional status of Cx43 as revealed by genetically modified mice. *Biochem J.* 2013; 449:401–413. [PubMed: 23075222]
31. Wang X, Ramirez A, Budunova I. Overexpression of connexin26 in the basal keratinocytes reduces sensitivity to tumor promoter TPA. *Exp Dermatol.* 2010; 19:633–640. co-expressed with Cx643 typical for basal and suprabasal keratinocytes As Cx626 gap junctional communication between keratinocytes and induce proliferation To generated transgenic mice using keratin635 promoter to target Cx626 to basal Cx643-positive keratinocytes We evaluated the effect of ectopic Cx626 on keratinocyte proliferation and differentiation in normal and 612-O-tetradecanoyl-phorbol-613-acetate (TPA)-treated skin The ectopic Cx626 keratinocyte differentiation and proliferation in newborn and adult skin decreased in epidermis of K635 Cx626 transgenics This correlated with significant down-regulation of TPA-induced activity of protein kinase C (PKC) in K635 Cx626 mice. [PubMed: 20002174]
32. Sonnenberg A, Daams H, Van der Valk MA, Hilkens J, Hilgers J. Development of mouse mammary gland: identification of stages in differentiation of luminal and myoepithelial cells using monoclonal antibodies and polyvalent antiserum against keratin. *J Histochem Cytochem.* 1986; 34:1037–1046. [PubMed: 2426332]
33. Daniel CW, Strickland P, Friedmann Y. Expression and functional role of E- and P-cadherins in mouse mammary ductal morphogenesis and growth. *Dev Biol.* 1995; 169:511–519. [PubMed: 7781895]
34. Raymond K, Cagnet S, Kreft M, Janssen H, Sonnenberg A, Glukhova MA. Control of mammary myoepithelial cell contractile function by alpha3beta1 integrin signalling. *EMBO J.* 2011; 30:1896–1906. [PubMed: 21487391]
35. El-Sabban ME, Sfeir AJ, Daher MH, Kalaany NY, Bassam RA, Talhouk RS. ECM-induced gap junctional communication enhances mammary epithelial cell differentiation. *J Cell Sci.* 2003; 116:3531–3541. [PubMed: 12893812]
36. Beyer EC, Gemel J, Martinez A, Berthoud VM, Valiunas V, Moreno AP, Brink PR. Heteromeric mixing of connexins: compatibility of partners and functional consequences. *Cell Commun Adhes.* 2001; 8:199–204. [PubMed: 12064588]
37. Willecke K, Kirchhoff S, Plum A, Temme A, Thonnissen E, Ott T. Biological functions of connexin genes revealed by human genetic defects, dominant negative approaches and targeted deletions in the mouse. *Novartis Found Symp.* 1999; 219:76–88. discussion 88–96. [PubMed: 10207899]
38. Monaghan P, Perusinghe NP, Cowen P, Gusterson BA. Peripubertal human breast development. *Anat Rec.* 1990; 226:501–508. [PubMed: 2331062]
39. McLachlan E, Shao Q, Laird DW. Connexins and gap junctions in mammary gland development and breast cancer progression. *J Membr Biol.* 2007; 218:107–121. [PubMed: 17661126]
40. Shao Q, Wang H, McLachlan E, Veitch GI, Laird DW. Down-regulation of Cx43 by retroviral delivery of small interfering RNA promotes an aggressive breast cancer cell phenotype. *Cancer Res.* 2005; 65:2705–2711. [PubMed: 15805269]
41. Dbouk HA, Mroue RM, El-Sabban ME, Talhouk RS. Connexins: a myriad of functions extending beyond assembly of gap junction channels. *Cell Commun Signal.* 2009; 7:4. [PubMed: 19284610]
42. Pauli BU, Augustin-Voss HG, el-Sabban ME, Johnson RC, Hammer DA. Organ-preference of metastasis. The role of endothelial cell adhesion molecules. *Cancer Metastasis Rev.* 1990; 9:175–189. [PubMed: 2292135]
43. Ito A, Katoh F, Kataoka TR, Okada M, Tsubota N, Asada H, Yoshikawa K, Maeda S, Kitamura Y, Yamasaki H, Nojima H. A role for heterologous gap junctions between melanoma and endothelial cells in metastasis. *J Clin Invest.* 2000; 105:1189–1197. [PubMed: 10791993]
44. el-Sabban ME, Pauli BU. Adhesion-mediated gap junctional communication between lung-metastatic cancer cells and endothelium. *Invasion Metastasis.* 1994; 14:164–176. [PubMed: 7657509]
45. Skerrett IM, Di WL, Kasperek EM, Kelsell DP, Nicholson BJ. Aberrant gating, but a normal expression pattern, underlies the recessive phenotype of the deafness mutant Connexin26M34T. *FASEB J.* 2004; 18:860–862. [PubMed: 15033936]

46. Iossa S, Marciano E, Franze A. GJB2 Gene Mutations in Syndromic Skin Diseases with Sensorineural Hearing Loss. *Curr Genomics*. 2011; 12:475–785. [PubMed: 22547955]
47. Bicego M, Beltramello M, Melchionda S, Carella M, Piazza V, Zelante L, Bukauskas FF, Arslan E, Cama E, Pantano S, Bruzzone R, D'Andrea P, Mammano F. Pathogenetic role of the deafness-related M34T mutation of Cx26. *Hum Mol Genet*. 2006; 15:2569–2587. [PubMed: 16849369]
48. Delmar M, Coombs W, Sorgen P, Duffy HS, Taffet SM. Structural bases for the chemical regulation of Connexin43 channels. *Cardiovasc Res*. 2004; 62:268–275. [PubMed: 15094347]
49. George CH, Kendall JM, Evans WH. Intracellular trafficking pathways in the assembly of connexins into gap junctions. *J Biol Chem*. 1999; 274:8678–8685. [PubMed: 10085106]
50. Evans WH, Ahmad S, Diez J, George CH, Kendall JM, Martin PE. Trafficking pathways leading to the formation of gap junctions. *Novartis Found Symp*. 1999; 219:44–54. discussion 54–49. [PubMed: 10207897]
51. Martin PE, Blundell G, Ahmad S, Errington RJ, Evans WH. Multiple pathways in the trafficking and assembly of connexin 26, 32 and 43 into gap junction intercellular communication channels. *J Cell Sci*. 2001; 114:3845–3855. [PubMed: 11719551]
52. Gemel J, Valiunas V, Brink PR, Beyer EC. Connexin43 and connexin26 form gap junctions, but not heteromeric channels in co-expressing cells. *J Cell Sci*. 2004; 117:2469–2480. [PubMed: 15128867]
53. Thomas T, Jordan K, Simek J, Shao Q, Jedeszko C, Walton P, Laird DW. Mechanisms of Cx43 and Cx26 transport to the plasma membrane and gap junction regeneration. *J Cell Sci*. 2005; 118:4451–4462. [PubMed: 16159960]
54. Giepmans BN, Verlaan I, Moolenaar WH. Connexin-43 interactions with ZO-1 and alpha- and beta-tubulin. *Cell Commun Adhes*. 2001; 8:219–223. [PubMed: 12064592]
55. Giepmans BN, Verlaan I, Hengeveld T, Janssen H, Calafat J, Falk MM, Moolenaar WH. Gap junction protein connexin-43 interacts directly with microtubules. *Curr Biol*. 2001; 11:1364–1368. [PubMed: 11553331]
56. Bascom JL, Fata JE, Hirai Y, Sternlicht MD, Bissell MJ. Epimorphin overexpression in the mouse mammary gland promotes alveolar hyperplasia and mammary adenocarcinoma. *Cancer Res*. 2005; 65:8617–8621. [PubMed: 16204027]

Highlights

Pups born to K5-Cx26 mothers die of starvation independent of their genotype.

The mammary glands of K5-Cx26 mice develop normally and produce milk.

K5-Cx26 dams are unable to eject milk after parturition.

Ectopic expression of Cx26 cells acts as a trans-dominant negative to endogenous Cx43.

Loss of Cx43 impairs oxytocin-mediated contraction in primary mammary organoids.

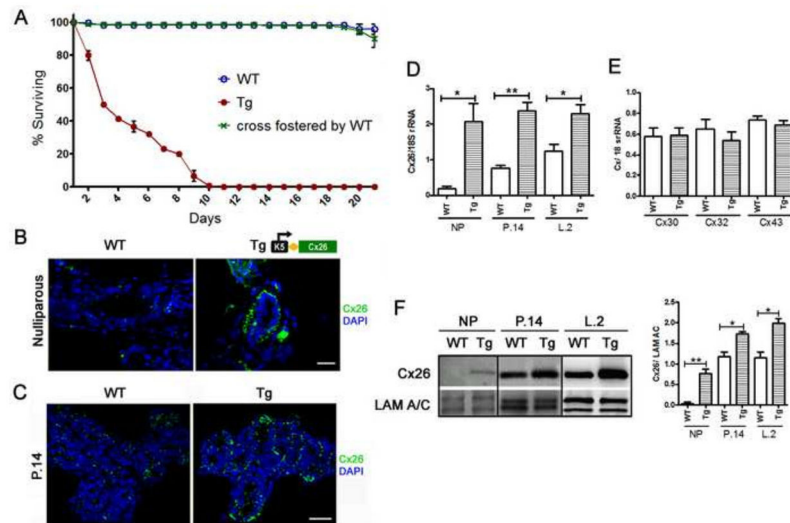


Figure 1. Ectopic expression of Cx26 in mammary myoepithelial cells correlates with starvation of pups born to K5-Cx26 dams

(A) Litters born to WT mothers have around 98–100% survival rate to weaning age (blue). Pups born to Tg mothers die from around day 4 to day 10 of lactation due to failure to thrive (red) but cross-fostering of pups born to Tg mothers by WT dams restores the survival rate to normal (blue and green) ($n=3$). (B) Staining for Cx26 (green) in mammary tissue sections from WT and Tg nulliparous littermates: Cx26 is localized to the basal cells in Tg mammary gland tissue sections, whereas no significant staining is observed in sections from WT mice. Scale bar 50 μ m. (C) Staining for Cx26 in tissue sections from mid-pregnant WT and Tg littermates confirms that Cx26 is expressed on the basal side of the mammary alveoli in the glands of Tg mice. Scale bars 20 μ m (D) Q-PCR analysis for the expression levels of Cx26 transcripts in nulliparous (NP), mid-pregnant at day 14 and early lactating at day 2 WT and Tg tissues normalized to 18S rRNA reveals increased expression in tissues from Tg mice ($n=3$, $p<0.03$, $p<0.005$, $p<0.03$ respectively). (E) Q-PCR analysis for the expression levels of mammary Cxs, Cx30, Cx32 and Cx43 reveals no differences in the levels of Cx mRNA in mammary glands of nulliparous Tg mice. (F) Western blot analysis of WT and Tg mammary gland homogenates at different time points of mammary development and corresponding quantification of Cx26 levels in comparison to Lamin A/C (LAM A/C) used as a loading control ($n=3$).

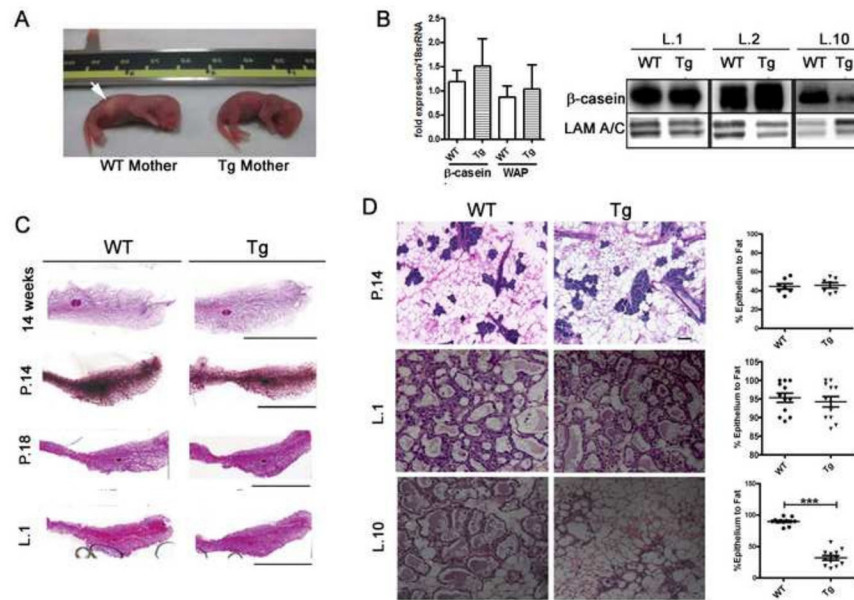


Figure 2. Milk delivery but not synthesis is impaired in the glands of K5-Cx26 dams despite normal development of the K5-Cx26 mammary glands

(A) Photograph of a pup born to a WT mother with milk spot in stomach (Arrow, pup on the left) and a pup born to Tg mother without a milk spot (right) reveals that pups born to Tg mothers do not receive milk. $n=10$ pairs of WT and Tg dams with variable litter sizes. (B) Q-PCR analysis for β -casein and WAP mRNA revealed no significant difference in the transcript levels in WT and Tg tissue in mid-pregnancy ($n=3$). Western blot analysis with anti- β -casein antibodies revealed that the protein was expressed comparably in WT and Tg tissues in early lactation, but β -casein levels drop significantly by day 10 of lactation in the glands of Tg mice, indicating early involution of the gland due to milk stasis. Equal loading was assessed using Lamin A/C. (C) Micrographs of stained whole mounts of mammary glands from WT and Tg mice at 14 week nulliparous mice, mid-pregnant (day 14), late pregnant (day 18) and early lactation (day 1) show no differences in gross size and structures of mammary glands from WT and Tg littermates at all stages examined scale bar 2cm. (D) H&E staining of tissue sections from the mammary glands of mid-pregnant (day 14), early lactating (day 2) and mid-lactating (day 10) of WT and Tg littermates and quantification of ratios of epithelial (purple/blue cells) compared to fat (adipose) cells (white and light pink). Scale bar 100 μ m. The difference in the epithelial/fat ratios between WT and Tg littermates at lactation day 10 are statistically significant ($p<0.0001$, $n=12$).

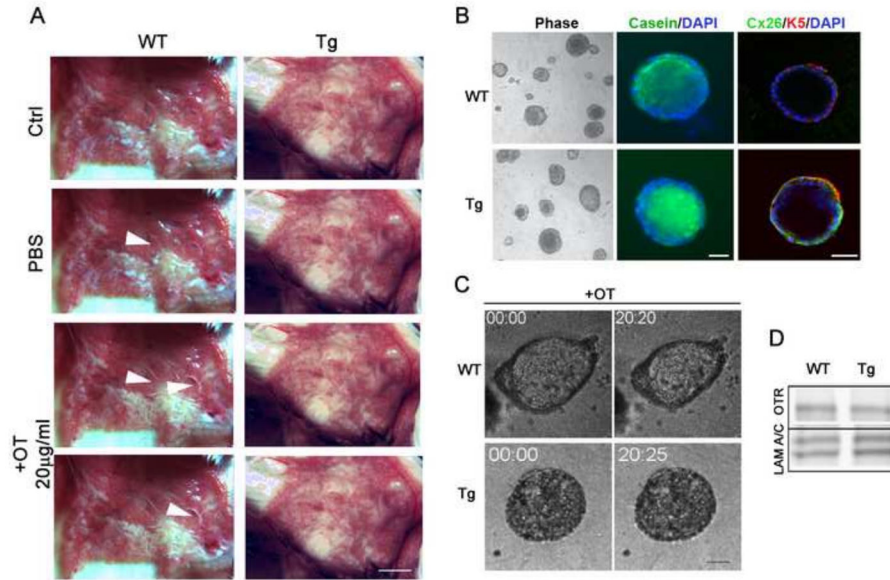


Figure 3. Mammary glands and organoids of K5-Cx26 females do not respond to oxytocin
 (A) Whole mammary glands from WT or Tg littermates were treated with PBS or PBS containing 20 µg/ml oxytocin *ex vivo* and the expulsion of milk into the ducts was evaluated. Arrowheads indicate release of milk into a duct after oxytocin exposure (n=4). Scale bar 1cm. (B) Primary organoids isolated from the glands of 6-week old virgin mice and cultured in differentiation medium that allow the production of β -casein were stained for Cx26 and β -casein expression. Phase contrast microscopy shows that organoids from WT and Tg mice appear similar in size. Fluorescence microscopy using anti β -casein antibodies, reveals that β -casein was produced and secreted vectorially into the lumen in WT and Tg organoids by day 4 of culture (Green). In addition and as expected, Cx26 (Green) localized with Keratin 5 (Red) in Tg organoids indicating myoep localization in Tg but not WT organoids. DAPI staining (blue) marks nuclei. (C) Oxytocin (10^{-6} i.u/ml) added on day 4 stimulated contraction (pulsing and decrease in size) in WT but not Tg organoid cultures. (D) OTR protein levels are not different in organoids isolated from the glands of WT and Tg mice indicating that the impaired response to oxytocin is not due to a defect in OTR expression. Scale bars 20 μ m. Lamin A/C was used for equal loading.

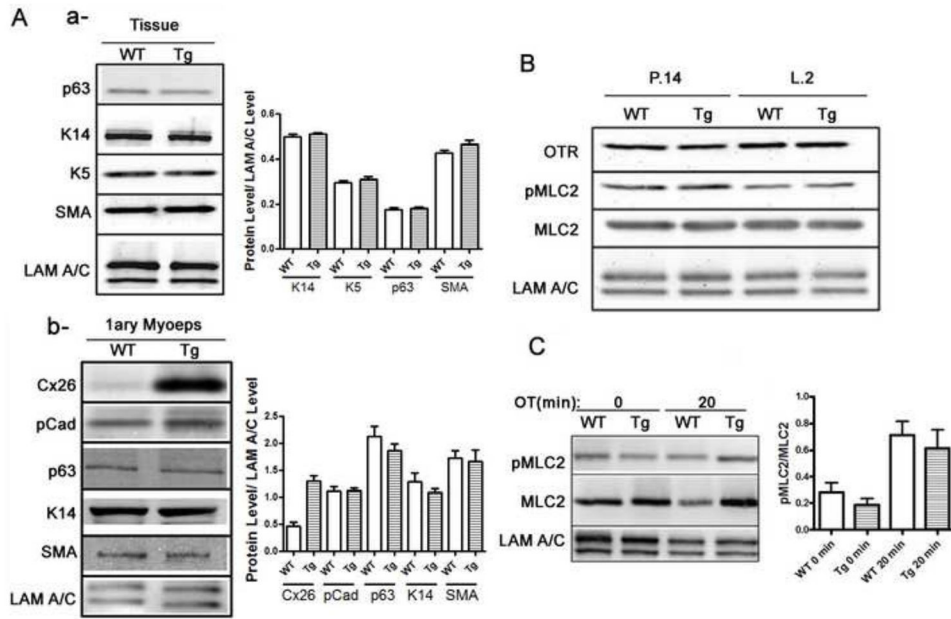


Figure 4. Mammary myoeps of Tg mice differentiate normally with no difference in intracellular signaling to the myosin light chain

(A) Western blot analysis of myoep-specific proteins in the mammary glands of WT and Tg littermates did not reveal significant differences. Densitometric analysis is provided (n=3) (a). Western blot analysis of myoep-specific proteins in the isolated myoeps did not reveal striking differences between WT and Tg cells. Densitometric analysis is provided (n=3) (b). (B) Western blot analysis of oxytocin receptor (OTR), myosin light chain 2 (MLC2) and phospho-myosin light chain 2 (pMLC2) in WT and Tg tissue of mid-pregnant and mid-lactating mice show no significant differences in the levels of the protein between WT and Tg littermates, suggesting that intracellular signaling from OTR is not compromised in the glands of Tg mice. (C) Western blot analysis of PMLC2 and MLC2 before and after (20') addition of oxytocin (OT) in primary organoids isolated from WT and Tg mice confirms that there are no significant differences in the ratios of PMLC2 to MLC2 between WT and Tg organoids before and after treatment with oxytocin (n=3).

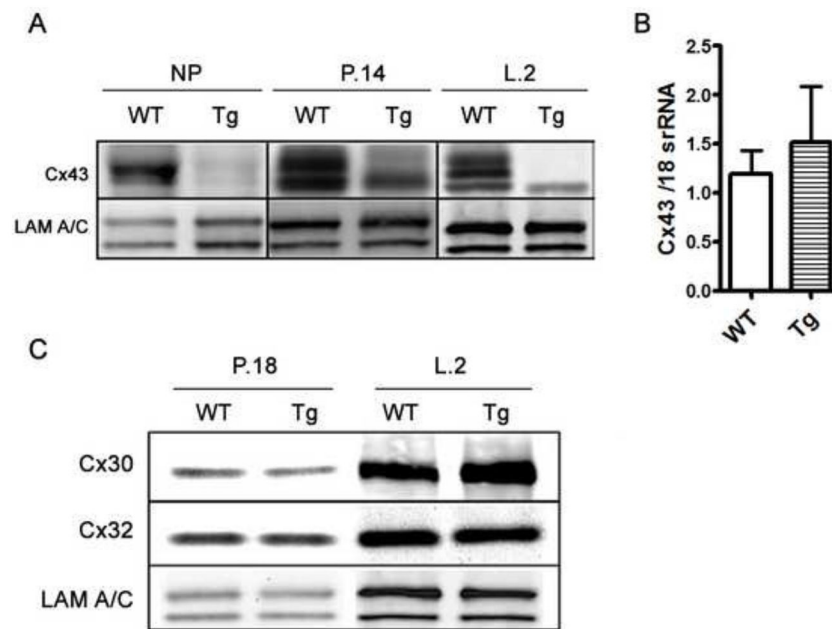


Figure 5. Cx26 acts as a trans-dominant negative to Cx43 in the glands of Tg mice
 (A) Western analysis on mammary protein samples across different time points revealed that during late pregnancy and early lactation, Cx43 levels are higher in wild type (WT) compared to transgenic (Tg) tissues. Lamin A/C is used for equal loading. (B) Q-PCR analysis of Cx43 transcript levels normalized to 18S rRNA (n=3) shows no significant difference in Cx43 mRNA levels in the glands of early lactating WT and Tg females. (C) Protein levels of Cx30 and C32 are similar in WT and Tg late pregnant and lactating littermates.

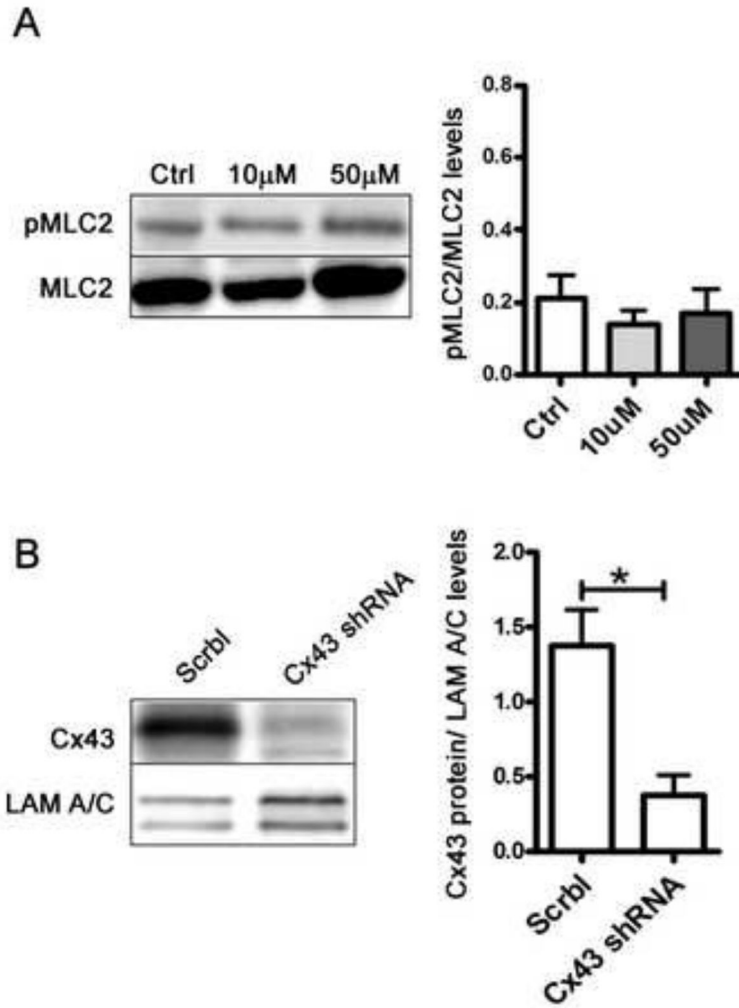


Figure 6. Defective gap junctional communication causes decreased mammary organoid contraction

(A) Western analysis of pMLC2 and MLC2 levels in primary organoids treated with gap junction inhibitor 18-alpha-Glycyrrhetic acid (18αGA) at concentrations of 10µM and 50µM reveals no differences in the ratios of pMLC2 to MLC2. (B) Western blot analysis confirming lower levels of Cx43 in WT organoids treated with Cx43 shRNA. Lamin A/C was used as a loading marker and Cx43 levels in WT organoids treated with scrambled shRNA (Scrbl) and Cx43shRNA.

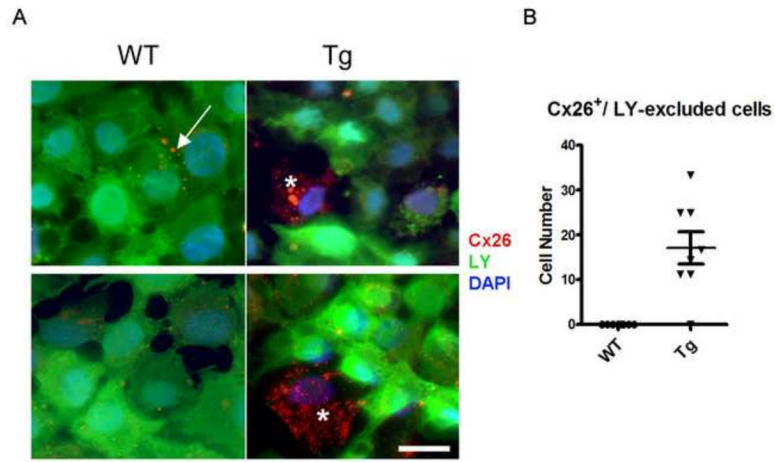


Figure 7. Cells from Tg mice with high Cx26 levels are impermeable to dye transfer
(A) Primary cells from WT and Tg mice were scraped and loaded with Lucifer Yellow (LY) dye to assess gap junctional communication. Dye spreading (green) is uniform across monolayers of primary mammary cells from WT mice, but dye spreading across monolayers of primary cells from Tg mice reveals that cells highly expressing Cx26 (red) are dye-excluded. Arrows point to Cx26 staining at the membrane in WT cells and asterisks denote cells that have high Cx26 and are dye excluded. (B) Total number of cells that have high levels of Cx26 and are dye excluded in primary cultures of mammary epithelial cells isolated from the glands of WT and Tg littermates.